tvst

Article

Comprehensive Proteomic Profiling of Aqueous Humor Proteins in Proliferative Diabetic Retinopathy

Hu Xiao[1,2,*], Wen Xin[2,*], Li Mei Sun[1], Song Shan Li[1], Ting Zhang[1], and Xiao Yan Ding[1]

[1] State Key Laboratory of Ophthalmology, Zhongshan Ophthalmic Center, Sun Yat-sen University, Guangzhou, Guangdong Province, China
[2] The 7th Affiliated Hospital of Sun Yat-sen University, Shenzhen, Guangdong Province, China

Correspondence: XiaoYan Ding, State Key Laboratory of Ophthalmology, Zhongshan Ophthalmic Center, Sun Yat-sen University, Guangzhou 510060, China. e-mail: dingxiaoyan@gzzoc.com

Received: December 3, 2020
Accepted: March 13, 2021
Published: May 4, 2021

Keywords: aqueous humor; proliferative diabetic retinopathy; diabetes mellitus; tandem mass tag; proteomics

Citation: Xiao H, Xin W, Sun LM, Li SS, Zhang T, Ding XY. Comprehensive proteomic profiling of aqueous humor proteins in proliferative diabetic retinopathy. Transl Vis Sci Technol. 2021;10(6):3, https://doi.org/10.1167/tvst.10.6.3

Purpose: Proliferative diabetic retinopathy (PDR) is a serious ocular disease that can lead to retinal microvascular complications in patients with diabetes mellitus. To date, no studies have explored PDR development by analyzing the aqueous humor (AH). Therefore we carried out tandem mass tag (TMT) proteomic quantification to compare AH protein profiles between PDR and non-PDR subjects.

Methods: We enrolled six PDR and six control (senile cataract) subjects. AH samples were collected during surgery and stored at −80°C. Proteins were extracted, trypsin-digested, and labeled with TMTs for mass spectrometric analysis.

Results: We found 191 proteins to be changed with $|\log_2 (\text{fold change})| \geq 1$ ($P < 0.05$ and identification with at least two peptides per protein). Of them, 111 were downregulated, whereas 80 were upregulated in the PDR group. Proteomic bioinformatic analysis indicated that PDR development was related to complement and coagulation cascades, platelet activation, extracellular matrix–receptor interaction, focal adhesion, protein digestion and absorption, human papillomavirus infection, PI3K-Akt signaling pathway, cholesterol metabolism, peroxisome proliferator-activated receptor signaling pathways, fat digestion and absorption, and vitamin digestion and absorption pathways.

Conclusions: Comprehensive proteomic profiling of the AH revealed 191 differentially expressed proteins between the two groups. Most of these proteins belong to secretory pathways, and therefore can be used as biomarkers in clinical testing and basic research.

Translational Relevance: Pathway analysis and a review of the literature enabled us to draw a novel biological map that will support further studies on the underlying mechanisms and therapeutic control of PDR development.

Introduction

Diabetes mellitus (DM) is a group of metabolic disorders associated with hyperglycemia, prevalent worldwide.[1,2] DM can lead to several macrovascular complications, such as cardiovascular disease, stroke, chronic kidney disease, foot ulcers, and damage to the nerves and eyes.[2] The ocular complications include keratitis, glaucoma, cataracts, and diabetic retinopathy (DR).[3,4] In turn, DR is the most common and serious ocular complication, causing progressive damage of the retinal microvasculature. Furthermore, proliferative diabetic retinopathy (PDR) is characterized by abnormal angiogenesis.[3,4]

Some pathophysiological mechanisms underlying the development of PDR have been proposed.[3–6] It is known that hyperglycemia is the onset factor of a number of pathological processes resulting in retinal abnormality. Hyperglycemia leads to microvascular injury, which can contribute to chronic inflammation and edema; these, in turn, can result in hypoxia and oxidative stress, which can then eventually lead to neurodegeneration and angiogenesis.[3] However, research on PDR lacks a comprehensive analysis; as a result, there are no clear biological maps to show the links among pathways that are important to the development of PDR.

Furthermore, although some studies have profiled the proteome of the vitreous humor (VH) associated

with PDR development,[5,6] only one has examined the proteome of the aqueous humor (AH).[4] In the latter, two-dimensional gel electrophoresis-tandem mass spectrometry (MS) analysis was used.[4] Eleven differentially expressed proteins were found in the AH associated with PDR. To our knowledge, our study is the first comprehensive proteomic profiling of the AH using tandem mass tag (TMT) proteomic quantification. TMT enables a more accurate and multiplexed quantification by MS for quantitative analysis.[7] Because the TMT reagent can label 11 samples after digestion, MS can concurrently detect 11 samples for quantification.[7] Thus this is a more accurate, high-throughput, and reliable technique than previous analytical approaches.

Methods

Study Design

Six PDR and six control (senile cataract) subjects were enrolled in this study. Written informed consent was obtained from all patients in the study. The study was performed in compliance with tenets of the Declaration of Helsinki for biomedical research and was approved by the Institutional Review Board of the Zhongshan Ophthalmic Center, Sun Yat-sen University, China. The enrollment criteria of the PDR group were as follows: (1) clinical diagnosis of PDR; (2) absence of other ocular diseases, pregnancy, or severe systemic conditions (except DM); and (3) absence of ocular treatment, such as photodynamic therapy, surgery, or intravitreal injection. For the control group, all six patients with senile cataract were scheduled for phacoemulsification cataract surgery for insertion of an intraocular lens. They had no history of other ocular diseases, prior intraocular treatment, and severe systemic conditions. Prior to AH collection, best corrected visual acuity (BCVA) and intraocular pressure (IOP) were measured.

AH Collection and Processing

Prior to intravitreal injection and incision, AH was collected during microscope-aided surgery using a sterile 1-mL insulin injection syringe with a needle. The samples were collected in a 1.5-mL microcentrifuge tube, quickly frozen on dry ice, and stored at –80°C until subsequent analyses. The samples were incubated on dry ice for not longer than 30 minutes.

Protein Extraction, Digestion, and Labeling

AH samples were sonicated three times on ice, using a high-intensity ultrasonic processor (Scientz, Ningbo, China), in lysis buffer containing a 1% protease inhibitor cocktail (Calbiochem, San Diego, CA) and 8 M urea. The remaining debris was removed by centrifugation at 12,000 × *g* and 4°C for 10 minutes. Further, supernatant was collected, and protein concentration was determined using the BCA Protein Assay Kit, according to the manufacturer's instructions. For digestion, the protein solution was reduced with 5 mM dithiothreitol for 30 minutes at 56°C and alkylated with 11 mM iodoacetamide for 15 minutes at 25°C in darkness. The protein sample was then diluted to a final urea concentration of less than 2 M by adding 100 mM triethylammonium bicarbonate (TEAB). Finally, trypsin was added at a 1:50 trypsin:protein mass ratio for the first digestion at 37°C overnight and at a 1:100 trypsin:protein mass ratio for a second 4-hour digestion.

After trypsin digestion, the peptides were desalted using a Strata-X C18 SPE column, and the eluate was vacuum-dried. The peptides were then reconstituted in 0.5 M TEAB and processed using TMT kit (11-plex, Thermo Fisher Scientific, Waltham, MA) according to the manufacturer's protocol. Briefly, one unit of TMT reagent was thawed and reconstituted in acetonitrile. The peptide mixtures were then incubated for 2 hours at room temperature, pooled, desalted, and dried by vacuum centrifugation.

MS Management

The tryptic peptides were fractionated by high pH reversed-phase High Performance Liquid Chromatography (HPLC) using an Agilent 300 Extend-C18 column (5 µm particles, 4.6 mm ID, 250 mm length). In brief, the peptides were first separated into 60 fractions using a gradient of 8% to 32% acetonitrile (pH 9.0) over 60 minutes. Then, the peptides were combined into 14 fractions and dried by vacuum centrifugation. The tryptic peptides were dissolved in 0.1% formic acid (solvent A) and directly loaded onto a homemade reversed-phase analytical column (15 cm length, 75 µm i.d.). The increasing gradient comprised 9% to 23% solvent B (0.1% formic acid in 98% acetonitrile) over 26 minutes, 23% to 35% solvent B over 8 minutes, and an increase to 80% solvent B in 3 minutes, before holding it at 80% for a final 3 minutes, all at a constant flow rate of 450 nL/min on an EASY-nLC 1000 Ultra Performance Liquid Chromatography (UPLC) system. The peptides were subjected to the nanospray ionization source followed by tandem MS/MS in Orbitrap Fusion coupled inline to the UPLC system. The electrospray voltage applied was 2.0 kV. The *m*/*z* scan range was 400 to 1500 for a full scan, and intact peptides were detected in Orbitrap at a resolution of

60,000. Peptides were then selected for MS/MS using an normalized collision energy (NCE) setting of 28, and the fragments were detected in Orbitrap at a resolution of 17,500. A data-dependent procedure was used, which alternated between 1 MS scan followed by 20 MS/MS scans with a 15.0-second dynamic exclusion. Automatic gain control was set as 5E4, and the fixed first mass was set as 100 *m/z*.

Data Analyses

The resulting MS/MS data were processed using MaxQuant search engine (v.1.5.2.8). Tandem mass spectra were searched against the human_swissprot database concatenated with a reverse decoy database. Trypsin/P was specified as the cleavage enzyme allowing up to two missing cleavages. The mass tolerance for precursor ions was set as 20 ppm in First search and 5 ppm in Main search, and that for fragment ions was set as 0.02 Da. Carbamidomethyl on Cys was specified as a fixed modification, and acetylation modification and oxidation on Met were specified as variable modifications. False discovery rate (FDR) was adjusted to <1%, and the minimum score for modified peptides was set as >40.

DAVID Gene Functional Classification Tool v6.8 (https://david.ncifcrf.gov/home.jsp) was used for protein functional classification and pathway analysis of differentially expressed proteins.

Statistical Analysis

The statistical analysis was performed using SPSS 23.0 (IBM Corporation, Armonk, NY). Parametric datasets were determined by independent *t*-test, whereas nonparametric datasets were analyzed by Mann–Whitney *U* test. Sex and patient numbers were calculated as percentages. The χ^2 analysis was applied when determining if sex was significantly different between treatment and control groups. Differentially expressed proteins were assessed by independent *t*-test and a fold change of PDR group relative to the control group. To control the number of false-positive results due to multiple testing, Benjamini–Hochberg procedure was used. A two-tailed *P* value <0.05 was accepted as statistically significant.

Results

Clinical Characteristics of Patients in the PDR and Control Groups

The clinical features of all patients in the PDR and control groups are summarized in Table 1. Overall, there were 12 patients enrolled in this study, 6 (50%) in the PDR group and 6 (50%) in the control group, including 5 (83.3%) women in the PDR group, and 4 (66.7%) in the control group ($P = 0.505$). The overall median age was 70 (56, 76.8) years, 57 (33.5, 64.5) years in the PDR group, and 76.5 (70.8, 78.8) years in the control group ($P = 0.009$). The overall average BCVA was 30.83 ± 18.32 letters. The BCVA of the PDR group was significantly worse than that of the control group (18.33 ± 16.02 vs. 43.33 ± 10.33, respectively; $P = 0.009$). There was no significant difference in IOP measurements between the PDR and control groups (PDR = 14.45 ± 1.76 mm Hg; control = 12.2 ± 2.17 mm Hg; $P = 0.078$).

Proteomic Analysis

Proteomic analysis identified 591 proteins with at least two peptides per protein and P <0.05. Of these, 191 were found to be changed by $|\log_2 (\text{fold change})| \geq 1$ (Fig. 1). Among the 191 proteins, 111 were downregulated, whereas 80 were upregulated in the PDR group compared with the control group. The 191 proteins were categorized using the Gene Ontology (GO) database (PANTHER classification system) based on their molecular function, biological process,

Table 1. Clinical Characteristics of the PDR and Control Groups

	Overall	PDR	Control	*P* Value
N	12	6 (50%)	6 (50%)	
Female (%)	9 (75%)	5 (83.3%)	4 (66.7%)	0.505[a]
Age (yr)	70 (56, 76.8)[d]	57 (33.5, 64.5)[d]	76.5 (70.8, 78.8)[d]	0.009[b]
BCVA	30.83 ± 18.32	18.33 ± 16.02	43.33 ± 10.33	0.009[c]
IOP (mm Hg)	13.33 ± 2.23	14.45 ± 1.76	12.2 ± 2.17	0.078[c]

[a] *P* value for χ^2 test.
[b] *P* value for Mann–Whitney *U* test.
[c] *P* value for independent *t*-test.
[d] Median (25th and 75th percentiles).

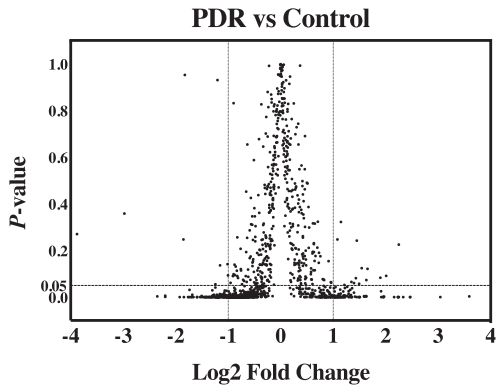

Figure 1. Volcano plot visualization of differentially expressed proteins. X-axis is the $\log_2$ of fold change (PDR group/control group). Y-axis is *P* value for independent *t*-test corrected by Benjamini–Hochberg procedure. Vertical dashed lines represent two-fold change in either direction (PDR/control or control/PDR). Horizontal dashed line represents a cutoff of *P* value 0.05. All 191 significantly differentially expressed proteins ($|\log2 \text{ (fold change)}| \geq 1$ and $P < 0.05$) fall to the left or right of vertical dashed lines and under the horizontal dashed line.

and cellular component (Fig. 2). Pathway analysis was performed using the DAVID Gene Functional Classification Tool. The PDR-associated pathways included complement and coagulation cascades, platelet activation, extracellular matrix (ECM)-receptor interaction, focal adhesion, protein digestion and absorption, human papillomavirus infection, the PI3K-Akt signaling pathway, cholesterol metabolism, peroxisome proliferator-activated receptor (PPAR) signaling pathway, fat digestion and absorption, and vitamin digestion and absorption pathways (Table 2).

Discussion

To our knowledge, this study is the first to use the TMT quantification approach for high-throughput profiling of differentially expressed proteins in the AH associated with the development of PDR. This high-throughput approach generated data for a more thorough protein–protein relationship network analysis to better understand the underlying mechanism of PDR development.

We used AH to indirectly explore the pathophysiologies underlying PDR. Balaiya et al.[8] have reported that differentially expressed proteins are similar between VH and AH in PDR compared with controls, and suggested that both VH and AH can be used in PDR studies. The differentially expressed proteins in VH may arise from the retina and seepage to AH by breaching the VH–AH barrier. In contrast, the retinal proteins may seep into AH by cilia-retinal circulation.[9] Further, a similar change of inflammatory cytokines in the VH and AH in PDR has been reported previously. Consequently, we consider that AH has the potential of replacing VH in PDR studies; this suggestion is supported by earlier reports.[8,10–12]

In this study, 111 proteins were found to be downregulated, whereas 80 proteins were upregulated in PDR AH. After GO categorization, the majority of the identified proteins were found to be extracellular or membrane proteins. This indicates that most proteins in the AH of patients with PDR were secreted proteins from the ciliary body and the ECM system. Secretory proteins can be used as biomarkers in clinical testing and ongoing research on the biological mechanism underlying PDR development.

Our bioinformatic analysis and thorough review of the literature estimated that the top 11 pathways are potentially related to PDR. Complement and coagulation cascades and platelet activation pathways share the same four proteins related to coagulation function: GFA, FGB, FGG, and ITGA2. Similarly, ECM-receptor interaction, focal adhesion, protein digestion and absorption, human papillomavirus infection, and the PI3K-Akt signaling pathway share the following proteins: COL2A1, COL9A1, COL9A2, SDC4, TNR, FN1, ITGA2, and VTN, which are related to the ECM. Cholesterol metabolism, the PPAR signaling pathway, fat digestion and absorption, and vitamin digestion and absorption pathways share APOA1, APOA4, and APOB, all of which function in lipid metabolism.

Complement and Coagulation Cascade-Related Pathways

After pathway analysis, 11 proteins were identified as being upregulated in complement and coagulation cascades in PDR. Among these, four proteins (C4BPA, C5, C9, and VTN) belong to complement cascades, and seven proteins (F13B, FGA, FGB, FGG, KLKB1, KNG1, and SERPIND1) are part of coagulation cascades. This finding shows a significant increase in complement and coagulation cascade activity in the AH during the development of PDR. Loukovaara et al.[6] and Schori et al.[5] reported that the complement and coagulation cascades could be upregulated in PDR in VH studies. Analysis of protein–protein interactions in the VH indicated that oxidative stress and apoptosis are potentially linked to the complement and coagulation cascades.[6] The upregulation of the latter may activate thrombosis, leukostasis, and inflammation processes.[6] These processes, in turn, may lead to edema and chronic inflammation in the development of PDR.

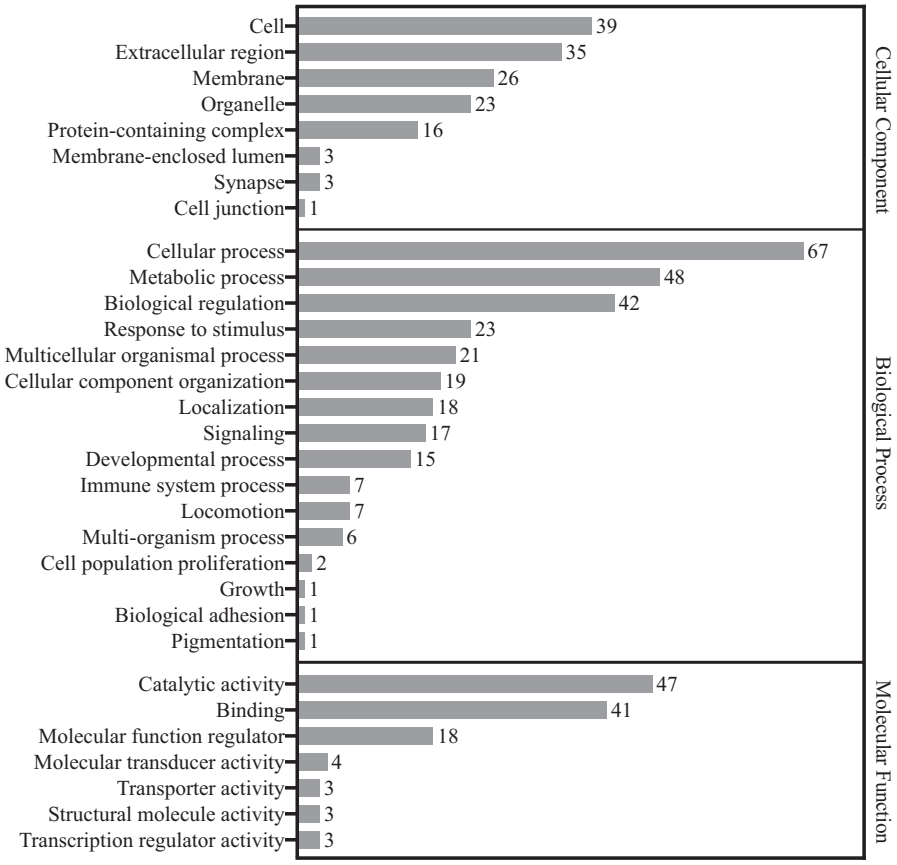

Figure 2. Gene Ontology analysis of the 191 significantly differentially expressed proteins between PDR and control groups. Bar charts represent the number of proteins associated to the GO terms, cellular component, biological process, and molecular function.

PI3K-Akt Signaling-Related Pathways

Proteins enriched in the PI3K-Akt signaling and ECM-receptor interaction pathways were found to be increased (FN1, ITGA2, and VTN) or decreased (COL2A1, COL9A1, COL9A2, and TNR) in PDR subjects. Most of these proteins are ECM proteins. The intracellular and extracellular microstructures are important to maintain retinal cell structure and function. Retinal blood vessel injury may lead to

Table 2. Top Pathways and Up- or Downregulated Proteins in the PDR Group

Pathway	Upregulated Proteins	Downregulated Proteins
Complement and coagulation cascades	C4BPA, C5, C9, F13B, FGA, FGB, FGG, KLKB1, KNG1, SERPIND1, VTN	
Platelet activation	FGA, FGB, FGG, ITGA2	
ECM-receptor interaction	FN1, ITGA2, VTN	COL2A1, COL9A1, COL9A2, SDC4, TNR
Focal adhesion	FN1, ITGA2, VTN	COL2A1, COL9A1, COL9A2, SDC4, TNR
Protein digestion and absorption	MEP1A	COL2A1, COL9A1, COL9A2
Human papillomavirus infection	FN1, ITGA2, VTN, MFNG	COL2A1, COL9A1, COL9A2, SDC4, TNR
PI3K-Akt signaling pathway	FN1, ITGA2, VTN	COL2A1, COL9A1, COL9A2, TNR
Cholesterol metabolism	APOA1, APOA2, APOA4, APOB, APOC1, APOC2, APOC3, LPA	LDLR, LRP2, SORT1
PPAR signaling pathway	ADIPOQ, APOA1, APOA2, APOC3, FABP1	
Fat digestion and absorption	APOA1, APOA4, APOB, FABP1	
Vitamin digestion and absorption	APOA1, APOA4, APOB	

changes in ECM proteins. Published reports have shown that changes in ECM proteins in the AH[4] and VH[6] are related to the development of PDR.

Moreover, in the PI3K-Akt signaling pathway, ECM proteins can promote integrin alpha 11 and then activate PI3K-Akt.[13,14] The PI3K-Akt signaling pathway can further upregulate the MAPK and VEGF signaling pathways, which can lead to cell proliferation and angiogenesis.[15,16] Our data showed that integrin alpha 11 significantly increased in the AH of PDR subjects and may initiate the development of PDR.

Cholesterol Metabolism-Related Pathways

Eight proteins involved in cholesterol metabolism and lipid-related metabolism, including APOA1, APOA2, APOA4, APOB, APOC1, APOC2, APOC3, and LPA, were increased in PDR subjects, and three proteins, including LDLR, LRP2, and SORT1, were decreased. Several studies have shown lipid-related metabolism being closely related to the development of PDR. Moosaie et al.[17] found serum Lp(a), APOA1, and APOB levels to be associated with PDR in a clinical study. Some proteomic studies have also shown differential lipid-related protein expression between PDR and non-PDR AH[4] and VH.[5,6] Moreover, high-density lipoproteins (HDLs) have been shown to promote the PI3K-Akt signaling pathway.[18,19] This may be the biological evidence of the involvement of lipid-related metabolism in PDR development.

Novel Biological Process Map Based on our Proteomic Data

Our database search and literature review indicated that insulin can promote the PI3K-Akt and MAPK signaling pathways.[20–22] In addition, ECM- and HDL-related proteins can activate the PI3K-Akt signaling pathway.[14,18,19]

The results presented here provide novel, essential insights toward the understanding of the underlying biological mechanisms of PDR development. The new biochemical targets identified in this study may aid the development of novel therapeutic interventions for PDR. Both the PI3K-Akt and MAPK signaling pathways can promote hypoxia-inducible factor 1 (HIF-1).[15,16,23] HIF-1 responds to hypoxia and upregulates the vascular endothelial growth factor (VEGF) signaling pathway.[15,16] In turn, VEGF initiates the mitogen–activated protein kinase (MAPK)signaling pathway, resulting in cell proliferation and angiogenesis.[15,16]

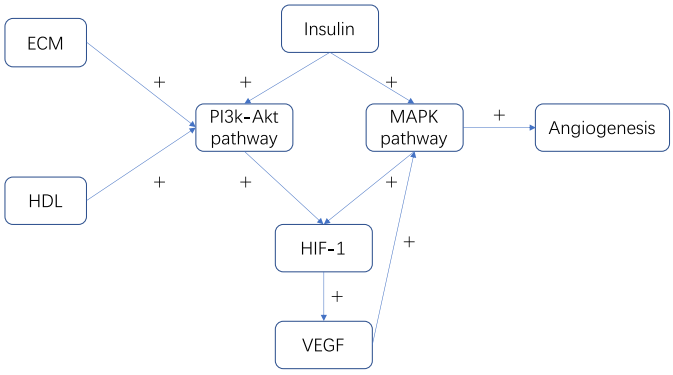

Figure 3. Novel biological process map for the development of PDR. Arrow represents direction of regulation and plus sign (+) represents upregulation or activation.

Overall, our pathway analysis and literature review enabled us to generate a novel biological process map for the development of PDR (Fig. 3). It is important to link the essential proteins and protein pathways together to use this knowledge as a reference in the study of the underlying mechanism of PDR in the future. In this map, it is apparent that the MAPK signaling pathway is presented downstream of VEGF and induces angiogenesis. The elucidation of the MAPK signaling pathway function may be the novel, key factor for the therapeutic control of angiogenesis in the development of PDR.

Although our study holds major implications, there are certain limitations associated as well. First, wet-lab experiments, such as western blot, enzyme-linked immunosorbent assays, multiple-reaction monitoring, or parallel-reaction monitoring MS, should have been performed to validate our study findings. Furthermore, it is better to perform in vivo experiments to determine the potential pathogenesis of PDR and therapeutic effects of the proteins as identified in the proposed novel biological process. Second, patients with senile cataract were enrolled as controls. Although senile cataract has no protopathy, proteins may change in the AH of patients with this condition. AH protein compositions are different between eyes with senile cataract and normal eyes. However, collection of AHs from normal eyes is not considered ethical. Therefore we chose and used AH from patients with senile cataract as control, concurrent with previously reported PDR proteomic studies.[24–26]

Conclusions

A comprehensive proteomic profiling of the AH revealed that 191 proteins were differentially expressed between PDR and control subjects. Most of these

proteins belong to secretory pathways, and therefore can be used as biomarkers in clinical testing and basic research. Eleven protein pathways were found to be upregulated or downregulated in PDR subjects compared with control subjects. Among these, complement and coagulation cascades, the PI3K-Akt signaling pathway, and cholesterol metabolism were the most highly represented pathways in PDR subjects. After pathway analysis and a thorough literature review, a novel biological process map was drawn to illustrate the protein–protein and pathway interactions, and further support studies on the underlying mechanism and therapeutic control of PDR development.

Acknowledgments

Supported by grants from the Fundamental Research Funds of the State Key Laboratory of Ophthalmology; research funds of the Sun Yat-sen University (15ykjc22d; Guangzhou, Guangdong, China); the Science and Technology Program Guangdong, China (2016A020215096; Guangzhou, Guangdong, China); and the Science and Technology Program Guangzhou, China (201803010031; Guangzhou, Guangdong, China).

Disclosure: **H. Xiao,** None; **W. Xin,** None; **L.M. Sun,** None; **S.S. Li,** None; **T. Zhang,** None; **X.Y. Ding,** None

[*] HX and WX contributed equally to the work and should therefore be regarded as equivalent first authors.

References

1. Wojciechowska J, Krajewski W, Bolanowski M, Krecicki T, Zatonski T. Diabetes and cancer: a review of current knowledge. *Exp Clin Endocrinol Diabetes*. 2016;124:263–275.
2. Rabiu MM, Taryam MO, Muhammad N, Oladigbolu K, Abdurahman H. Prevalence of diabetes mellitus and diabetic retinopathy in persons 50 years and above in Katsina State Nigeria: a population-based cross-sectional survey. *Ophthalmic Epidemiol*. 2020;27(5):384–389.
3. Negi A, Vernon SA. An overview of the eye in diabetes. *J R Soc Med*. 2003;96:266–272.
4. Chiang SY, Tsai ML, Wang CY, et al. Proteomic analysis and identification of aqueous humor proteins with a pathophysiological role in diabetic retinopathy. *J Proteom*. 2012;75:2950–2959.
5. Schori C, Trachsel C, Grossmann J, Zygoula I, Barthelmes D, Grimm C. The proteomic landscape in the vitreous of patients with age-related and diabetic retinal disease. *Invest Ophthalmol Vis Sci*. 2018;59:AMD31–AMD40.
6. Loukovaara S, Nurkkala H, Tamene F, et al. Quantitative proteomics analysis of vitreous humor from diabetic retinopathy patients. *J Proteome Res*. 2015;14:5131–5143.
7. Zecha J, Satpathy S, Kanashova T, et al. TMT labeling for the masses: a robust and cost-efficient, in-solution labeling approach. *Mol Cell Proteomics*. 2019;18:1468–1478.
8. Balaiya S, Zhou Z, Chalam KV. Characterization of vitreous and aqueous proteome in humans with proliferative diabetic retinopathy and its clinical correlation. *Proteomics Insights*. 2017;8:1178641816686078.
9. Freddo TF. A contemporary concept of the blood-aqueous barrier. *Prog Retin Eye Res*. 2013;32:181–195.
10. Wu F, Phone A, Lamy R, et al. Correlation of aqueous, vitreous, and plasma cytokine levels in patients with proliferative diabetic retinopathy. *Invest Ophthalmol Vis Sci*. 2020;61:26.
11. Rocha AS, Santos FM, Monteiro JP, et al. Trends in proteomic analysis of human vitreous humor samples. *Electrophoresis*. 2014;35:2495–2508.
12. Li J, Lu Q, Lu P. Quantitative proteomics analysis of vitreous body from type 2 diabetic patients with proliferative diabetic retinopathy. *BMC Ophthalmol*. 2018;18:151.
13. Bayer ML, Svensson RB, Schjerling P, Williams AS, Wasserman DH, Kjaer M. Influence of the integrin alpha-1 subunit and its relationship with high-fat diet upon extracellular matrix synthesis in skeletal muscle and tendon. *Cell Tissue Res*. 2020;381(1):177–187.
14. Ruiz-Ojeda FJ, Mendez-Gutierrez A, Aguilera CM, Plaza-Diaz J. Extracellular matrix remodeling of adipose tissue in obesity and metabolic diseases. *Int J Mol Sci*. 2019;20:4888.
15. Polivka J, Jr., Janku F. Molecular targets for cancer therapy in the PI3K/AKT/mTOR pathway. *Pharmacol Ther*. 2014;142:164–175.
16. Hybel TE, Dietrichs D, Sahana J, et al. Simulated microgravity influences VEGF, MAPK, and PAM signaling in prostate cancer cells. *Int J Mol Sci*. 2020;21:1263.
17. Moosaie F, Davatgari RM, Firouzabadi FD, et al. Lipoprotein(a) and apolipoproteins as predictors for diabetic retinopathy and its severity in adults with type 2 diabetes: a case-cohort study. *Can J Diabetes*. 2020:44(5):414–421.

18. Durham KK, Chathely KM, Trigatti BL. High-density lipoprotein protects cardiomyocytes against necrosis induced by oxygen and glucose deprivation through SR-B1, PI3K, and AKT1 and 2. *Biochem J*. 2018;475:1253–1265.
19. Theofilatos D, Fotakis P, Valanti E, Sanoudou D, Zannis V, Kardassis D. HDL-apoA-I induces the expression of angiopoietin like 4 (ANGPTL4) in endothelial cells via a PI3K/AKT/FOXO1 signaling pathway. *Metabolism*. 2018;87:36–47.
20. Liu S, Gao F, Wen L, et al. Osteocalcin induces proliferation via positive activation of the PI3K/Akt, P38 MAPK pathways and promotes differentiation through activation of the GPRC6A-ERK1/2 pathway in C2C12 myoblast cells. *Cell Physiol Biochem*. 2017;43:1100–1112.
21. Cui X, Qian DW, Jiang S, Shang EX, Zhu ZH, Duan JA. Scutellariae radix and coptidis rhizoma improve glucose and lipid metabolism in T2DM rats via regulation of the metabolic profiling and MAPK/PI3K/Akt signaling pathway. *Int J Mol Sci*. 2018;19:3634.
22. Mehta RJ, Gastaldelli A, Balas B, Ricotti A, DeFronzo RA, Tripathy D. Mechanism of action of inhaled insulin on whole body glucose metabolism in subjects with type 2 diabetes mellitus. *Int J Mol Sci*. 2019;20:4230.
23. Voest EE. Inhibitors of angiogenesis in a clinical perspective. *Anticancer Drugs*. 1996;7:723–727.
24. Vujosevic S, Micera A, Bini S, Berton M, Esposito G, Midena E. Proteome analysis of retinal glia cells-related inflammatory cytokines in the aqueous humour of diabetic patients. *Acta Ophthalmol*. 2016;94:56–64.
25. Zhang H, Liang L, Huang R, Wu P, He L. Comparison of inflammatory cytokines levels in the aqueous humor with diabetic retinopathy. *Int Ophthalmol*. 2020;40:2763–2769.
26. Mao D, Peng H, Li Q, et al. Aqueous humor and plasma adiponectin levels in proliferative diabetic retinopathy patients. *Curr Eye Res*. 2012;37:803–808.